

Synthesis and Photophysical Properties of Zeolite-Entrapped Bisterpyridine Ruthenium(II). Dramatic Consequences of Ligand-Field-State Destabilization

Anwar A. Bhuiyan and James R. Kincaid*

Chemistry Department, Marquette University, Milwaukee, Wisconsin 53201-1881

Received July 31, 1997

A bisterpyridine complex of ruthenium(II) ($\text{Ru}(\text{tpy})_2^{2+}$) has been prepared in zeolite Y supercages and investigated by electronic absorption, electronic emission, and resonance Raman spectroscopy. In free solution this complex is practically nonluminescent, having a very short excited-state lifetime (250 ps) at room temperature. However, entrapment within the zeolite supercage results in dramatic increases in emission intensity and excited-state lifetime (140 ns) at room temperature. The observed temperature dependence of the excited-state lifetime has been modeled by a kinetic equation with two thermal terms corresponding to the so-called fourth $^3\text{MLCT}$ state and ligand-field state (LF), respectively. It is shown that the increased lifetime of the entrapped complex results from zeolite-induced destabilization of the LF state, a conclusion which is in agreement with results obtained for a number of other zeolite-entrapped ruthenium(II) polypyridine complexes.

Introduction

The study of the photophysical and photochemical properties of transition metal complexes is of great interest for a variety of fundamental and practical reasons. In the past few years most of the attention in this field has been focused on the polypyridine complexes of ruthenium(II) as components of solar energy conversion schemes.¹ This has prompted several research groups^{2–5} to investigate the properties of these complexes entrapped within the supercages of Y-zeolite.

The results of detailed studies of the photophysical properties of a range of zeolite-entrapped complexes demonstrated that the most important effect of entrapment of such complexes within the Y-zeolite supercages is to increase the energy of the so-called “ligand field” (^3dd) state.^{5c} Thus, in the case of Z-Ru-(bpy)₂(daf)²⁺ (where daf is diazafluorene), the complex is essentially nonemitting in free solution owing to its very low lying ^3dd state.^{6a} Upon incorporation into the zeolite supercage, the complex exhibits easily detectable emission and a dramati-

cally increased $^3\text{MLCT}$ state lifetime (300 ns at room temperature), implying that the ^3dd state has indeed been destabilized by entrapment.^{5c} Specifically, a thorough analysis of data from extensive temperature-dependent lifetime studies reveals that the $^3\text{MLCT}$ – ^3dd state energy gap increased from $\sim 2300\text{ cm}^{-1}$ for the free complex to $\sim 4000\text{ cm}^{-1}$ in the case of the entrapped species.^{5c}

The above referenced study, demonstrating the effectiveness of zeolite entrapment in eliminating the LF state destabilization pathway, prompted us to undertake the study of zeolite entrapped complexes of terpyridine (tpy). In free solution the bis-tpy complex, $\text{Ru}(\text{tpy})_2^{2+}$, is essentially nonluminescent, having a very short lifetime ($\sim 250\text{ ps}$)^{6b} at room temperature. The origin of this short lifetime has been debated. In an early work, Meyer and co-workers⁷ attributed this short lifetime to enhanced nonradiative decay due to solvent interactions. However, from later studies, the short lifetime was attributed to thermally activated, nonradiative decay via metal-centered dd excited states.^{8–10} Meyer and co-workers⁸ showed that the vibrational characteristics of tpy as the acceptor ligand also influence nonradiative decay. Calzaferri and co-workers¹¹ explained this short lifetime at room temperature as being due to efficient decay through low-energy intramolecular vibrations of the nonrigid tpy complex and not to the coupling with dd states. According to this explanation, lowering the temperature results in “freezing” the intramolecular movements and significantly increasing the luminescence quantum yield. Meyer, Rillema, and co-workers¹² have shown that the nonradiative decay from the $^3\text{MLCT}$ states of these types of complexes is governed by the

- (1) (a) Jures, A.; Balzani, V.; Barigelletti, F.; Champagna, S.; Belsler, P.; von Zalewsky, A. *Coord. Chem. Rev.* **1988**, *84*, 85. (b) Kalyanasundaram, K. *Photochemistry of Polypyridine and Porphyrin Complexes*; Academic Press Limited: London, England, 1992.
- (2) (a) DeWilde, W.; Peeters, G.; Lunsford, J. H. *J. Phys. Chem.* **1980**, *84*, 2306. (b) Quayle, W. H.; Lunsford, J. H. *Inorg. Chem.* **1982**, *21*, 97.
- (3) (a) Dutta, P. K.; Incavo, J. A. *J. Phys. Chem.* **1987**, *91*, 4443. (b) Incavo, J. A.; Dutta, P. K. *J. Phys. Chem.* **1990**, *94*, 3075. (c) Turbeville, W.; Robins, D. S.; Dutta, P. K. *J. Phys. Chem.* **1992**, *96*, 5024. (d) Dutta, P. K.; Turbeville, W. *J. Phys. Chem.* **1992**, *96*, 9410. (e) Borja, M.; Dutta, P. K. *Nature* **1993**, *362*, 43.
- (4) Li, Z.; Wang, C. H.; Persaud, L.; Mallouk, T. E. *J. Phys. Chem.* **1988**, *92*, 2592. (b) Kruger, J. S.; Mayer, J. A.; Mallouk, T. E. *J. Am. Chem. Soc.* **1988**, *110*, 8232. (c) Kim, Y.; Mallouk, T. E. *J. Phys. Chem.* **1992**, *96*, 2879.
- (5) (a) Maruszewski, K.; Strommen, D. P.; Handrich, K.; Kincaid, J. R. *Inorg. Chem.* **1991**, *30*, 4595. (b) Maruszewski, K.; Strommen, D. P.; Kincaid, J. R. *J. Am. Chem. Soc.* **1993**, *115*, 8345. (c) Maruszewski, K.; Kincaid, J. R. *Inorg. Chem.* **1995**, *34*, 2002. (d) Szulbinski, W. S.; Kincaid, J. R. *Inorg. Chem.*, in press.
- (6) (a) Henderson, L. J., Jr.; Fronczek, F. R.; Cherry, W. R. *J. Am. Chem. Soc.* **1984**, *106*, 5876. (b) Winkler, J. R.; Netz, T. L.; Creutz, C.; Sutin, N. *J. Am. Chem. Soc.* **1987**, *109*, 2381.

- (7) Young, R. C.; Nagle, J. K.; Meyer, T. J.; Whitten, D. G. *J. Am. Chem. Soc.* **1978**, *100*, 4773.
- (8) Coe, B. J.; Thompson, D. W.; Culbertson, C. D.; Schoonover, J. R.; Meyer, T. J. *Inorg. Chem.* **1995**, *34*, 3385.
- (9) Clark, R. H.; Ann, K. I. G.; David, R. M. *Inorg. Chem.* **1991**, *30*, 538.
- (10) Kirchhoff, J. R.; McMillin, D. R.; Marnot, P. A.; Sauvage, J. P. *J. Am. Chem. Soc.* **1985**, *107*, 1138.
- (11) Amouyal, E.; Bahout, M. M.; Calzaferri, G. *J. Phys. Chem.* **1991**, *95*, 7641.

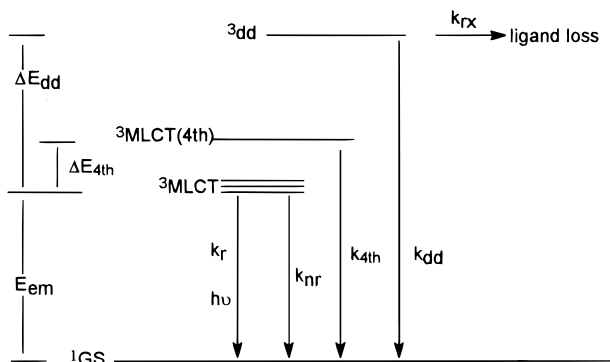


Figure 1. Schematic representation of the excited-state deactivation pathways in ruthenium-polypyridine complexes.

energy gap law, and for most of them the 3dd state is sufficiently low in energy so as to dominate the thermal contribution to the overall relaxation rate. It has been demonstrated that entrapment of such complexes within zeolite-Y supercages⁵ apparently eliminates this decay route by increasing the magnitude of ΔE_1 . This 3dd state destabilization presumably arises as a consequence of steric restrictions imposed by the fixed size of the supercage, an effect similar to that observed by Meyer and co-workers in rigid matrixes.^{12b} The actual values of the rate constants and energy gaps shown in Figure 1 can be experimentally determined by conducting lifetime measurements over a wide range of temperatures, as explained fully in refs 5b and 12a,b.

In this paper we report the results of such a study of the bisterpyridine complex of ruthenium(II) entrapped within zeolite supercages. The results of this study reveal that the increased LF state destabilization in this complex is comparable to that observed upon zeolite-Y-entrapped $\text{Ru}(\text{bpy})_2\text{daf}^{2+}$ ^{5c} and nicely demonstrate the concept that zeolite entrapment provides a quite useful strategy for advantageous manipulation of the photo-physical properties of such systems.

Experimental Section

A. Materials. The Y-zeolite, 2,2':6',2''-terpyridine(tpy), $\text{Ru}(\text{NH}_3)_6\text{Cl}_3$, $\text{RuCl}_3 \cdot \text{H}_2\text{O}$, and *N*-ethylmorpholine were purchased from the Aldrich Chemical Co. (Milwaukee, WI). The zeolite sample was purified by calcination^{3b} and washed with a 10% NaCl solution and deionized water. The ligand was sublimed prior to use, and the other chemicals were used without further purification. All solvents used were reagent grade or better. $[\text{Ru}(\text{NH}_3)_5\text{H}_2\text{O}]^{2+}$ was prepared by literature methods.¹³

B. Preparation of Compounds. 1. From $\text{Ru}(\text{NH}_3)_6\text{Cl}_3$. The zeolite entrapped complex $\text{Z-Ru}(\text{tpy})_2^{2+}$ was prepared by a modification of a method previously developed in our laboratory,^{5a} which is based on the pioneering work of Lunsford and co-workers.^{2a,b} Briefly, the pH of a water suspension of calcined zeolite (2.0 g) was adjusted to ~ 5.5 and then the appropriate amount of $\text{Ru}(\text{NH}_3)_6\text{Cl}_3$ (depending on desired load of $\text{Ru}(\text{tpy})_2^{2+}$) was ion-exchanged overnight. The ion-exchanged zeolite was separated by filtration and dried under vacuum. A 50-fold excess of the tpy ligand (with respect to $\text{Ru}(\text{NH}_3)_6^{3+}$) was added and mixed. The mixture was then transferred to a reaction tube fitted with a vacuum stopcock. The tube was filled with nitrogen and evacuated three times. The evacuated tube was then partially immersed in an oil bath and heated at 180–200 °C for 24 h. The product was

washed with 10% (w/v) NaCl solution, DI water, and 95% ethanol and then was Soxhlet extracted to remove the excess ligand. Spectroscopic measurements indicated that $\text{Z-Ru}(\text{tpy})_2^{2+}$ was formed, but the sample was contaminated by a species which absorbs near 552 nm.

2. From $[\text{Ru}(\text{NH}_3)_5\text{H}_2\text{O}]^{2+}$. A modification of the above procedure was undertaken, wherein the zeolite was ion-exchanged with $[\text{Ru}(\text{NH}_3)_5\text{H}_2\text{O}]^{2+}$. The calcined zeolite sample was degassed at 160 °C overnight, and then degassed acetone (4 times FPT) was distilled into the flask containing the zeolite. $[\text{Ru}(\text{NH}_3)_5\text{H}_2\text{O}]^{2+}$ was added under an argon atmosphere and allowed to ion-exchange for 90 min. Acetone was evaporated by blowing Ar at 60 °C, the flask was then taken into the glovebox and filled with argon, and the tpy ligand was added. The procedures described above were then followed for the remainder of the synthesis. The zeolite-entrapped complex was extracted from the zeolite matrix by the hydrofluoric acid method described in ref 5a. The integrity of the zeolite-entrapped sample was confirmed by RR, electronic absorption, and emission spectra. The free $\text{Ru}(\text{tpy})_2^{2+}$ complex was prepared by literature methods.¹⁴

C. Spectroscopic Measurements. 1. Electronic Absorption Spectra. Electronic absorption spectra were obtained with a Hewlett-Packard model 8452A diode array spectrometer. Solid samples were mixed with a few drops of mineral oil, and the resulting paste was diluted with additional oil and placed in a 1-cm quartz cuvette. Spectra were obtained in the absorbance mode. The diffuse reflectance spectra were recorded on Perkin-Elmer 320 scanning spectrometer equipped with a Hamamatsu integrating sphere attachment. For these measurements, a plain Na–Y-zeolite sample was used as a blank and finely ground BaSO_4 was used as a reference. The spectra were recorded in the transmittance mode and then numerically Kubelka–Munk¹⁵ corrected using the facilities of SpectraCalc software.

2. Ground-State Resonance Raman Spectra. Spectra were obtained with a conventional Raman spectrometer (Spex model 1403 double monochromator equipped with a Spex model DMIB controller and Hamamatsu R928 photomultiplier tube) with 476.5 nm excitation from a Spectra-Physics model 2025-05 argon ion laser. Spectra of the zeolite-entrapped compound were obtained from solid samples in a rotating NMR tube. Spectra of the free compound were obtained from an acetonitrile solution in the same manner. The absorption spectra were the same before and after RR measurements, indicating that there was no significant photodecomposition upon exposure to laser excitation. The spinning 5 mm i.d. NMR tube was illuminated by a laser beam focused through a glass lens, and the scattered light was collected with a conventional two-lens collection system.

3. Electronic Emission Spectra. The spectroscopic apparatus was the same as for the ground-state Raman measurements. Typically, 457.9 or 476.5 nm excitation was focused onto the spun NMR tube containing solid samples of the zeolite-entrapped complex. In the case of emission measurements at 77 K, the spinning NMR tube was positioned into a double-walled glass Dewar cell holder whose coolant reservoir was filled with liquid nitrogen. Spectra of the compound extracted from the zeolite matrix were obtained from a water solution, and that of the free complex was obtained from a butyronitrile solution.

4. Excited State Lifetimes. The third harmonic (354.7 nm) of a Quanta-Ray (Spectra-Physics) model GCR-11 Nd:YAG laser (operated at 20 Hz) with the beam defocused was used as the excitation source for the lifetime measurements. The emitted light was transferred through collecting and transferring lenses to a SPEX 340S spectrometer equipped with an RCA C31034A-02 photomultiplier tube. The photomultiplier tube output signal was directed to a Lecroy 9450A dual 300-MHz oscilloscope. Typically 500 scans of the emission decay curve were averaged and transferred to the computer. The emission decay curves were then fitted to a biexponential model using commercial software (PSI-Plot) based on the Marquardt–Levenberg algorithm.¹⁶

(12) (a) Allen, G. H.; White, R. P.; Rillema, D. P.; Meyer, T. J. *J. Am. Chem. Soc.* **1984**, *106*, 2613. (b) Lumpkin, R. S.; Kober, M. E.; Worl, L. A.; Murtaza, Z.; Meyer, T. J. *J. Phys. Chem.* **1990**, *94*, 239. (c) Rillema, D. P.; Blanton, C. B.; Shaer, R. J.; Jackman, D. C.; Boldaji, M.; Bundy, S.; Worl, L. A.; Meyer, T. J. *Inorg. Chem.* **1992**, *31*, 1600. (d) Barqawi, K. R.; Llobet, A.; Meyer, T. J. *J. Am. Chem. Soc.* **1988**, *110*, 7751. (e) Caspar, J. V.; Meyer, T. J. *Inorg. Chem.* **1983**, *22*, 2444.

(13) Kuehn, C. G.; Taube, H. *J. Am. Chem. Soc.* **1976**, *98*, 689.

(14) Maestri, M.; Armaroli, N.; Balzani, V.; Constable, E. C.; Thompson, A. M. W. *C. Inorg. Chem.* **1995**, *34*, 2759.

(15) Kubelka, P. *J. Opt. Soc. Am.* **1948**, *38*, 448.

(16) Marquardt, D. W. *J. Soc. Ind. Appl. Math.* **1963**, *11*, 431.

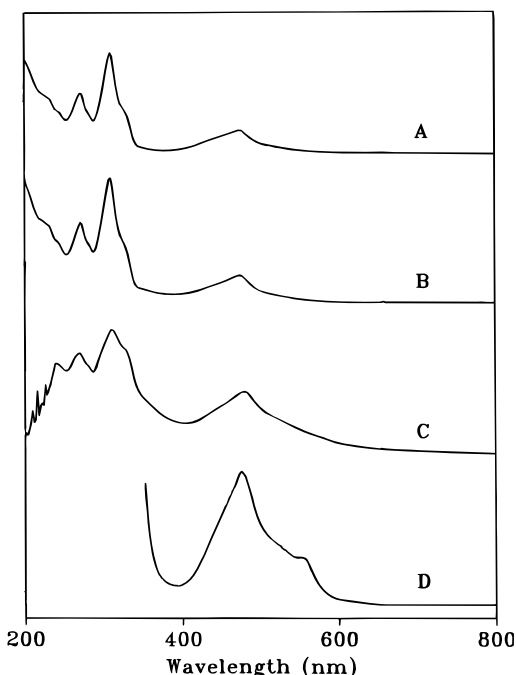


Figure 2. Electronic absorption spectra of $\text{Ru}(\text{tpy})_2^{2+}$: independently synthesized complex (trace A); extracted from zeolite (trace B); Nujol suspension of zeolite-entrapped complex (trace C); and diffuse reflectance spectrum of the zeolite-entrapped complex (trace D).

The temperature-dependent lifetime measurements were acquired with the aid of a cold cell of in-house design, which consists of a Dewar containing an NMR tube spinner. The Dewar was filled with ethanol/liquid nitrogen cooling mixture, and an NMR tube containing the zeolite sample was then immersed. The sample temperature was allowed to equilibrate for at least 10 min, and, as the temperature of the cooling mixture was allowed to rise slowly, the decay curves were measured at various temperatures. The temperature inside the Dewar was measured using a TEGAM 821 microprocessor thermometer equipped with thermocouple. The temperature variations during the collection of the data (500 sweeps/25 s) was approximately 0.5–0.6 °C. The average value was considered as the experimental temperature for the measurement.

Results

A. Electronic Absorption and Emission Spectra. The electronic absorption and emission spectra of the complex in various forms are given in Figures 2 and 3. The absorption spectrum of the independently synthesized complex in acetonitrile solution, given in trace A, Figure 2, matches that reported in the literature.¹⁴ The absorption spectrum of the zeolite-entrapped complex (trace C), as well as the liberated complex which is obtained following dissolution of the zeolite matrix (trace B), show no significant differences in the positions of the absorption maxima compared to the spectrum of the independently prepared solution phase complex. Figure 3 shows evidence of a slight red shift (10 nm) for the zeolite-entrapped species, a result which is consistent with the results reported previously for other zeolite-entrapped species.^{5b}

B. Resonance Raman (RR) Spectra. The RR spectra of the complex in solution and that of the zeolite-entrapped species are given in Figure 4. The spectral pattern does not significantly change upon entrapment of the complex into the zeolite matrix. There are only slight shifts ($\leq 7 \text{ cm}^{-1}$) observed for the zeolite-entrapped complex relative to the solution phase complex.

C. Lifetime Data. The ³MLCT state lifetime of $\text{Ru}(\text{tpy})_2^{2+}$ in solutions is too short (250 ps^{6b} at room temperature) to be

recorded on the (nanosecond time scale) equipment available to us. However, the luminescence of the zeolite-entrapped sample at room temperature has an associated lifetime of 140 ns in aqueous suspension. As in the case of some other zeolite-entrapped complexes,^{3c,5b,c} it was necessary to apply a biexponential model of the decay to reproduce the observed decay curves, with a short-lived (~ 35 ns) component (presumably attributable to a small fraction of interacting adjacent-case pairs)^{17b} contributing approximately 14% of the initial emission intensities. Excited-state lifetimes obtained at low temperatures increase, as expected, with decreasing temperature, reaching 844 ns at -50 °C accompanied by a short-living component of 170 ns (4% of the initial intensities). Figure 5 presents semilogarithmic plots of the decay curves obtained at room temperature and -50 °C.

Discussion

A. Synthesis. The sample was contaminated by a species that absorbs near 552 nm (shown in Figure 2d) when the synthesis was conducted using zeolite containing ion-exchanged $\text{Ru}(\text{NH}_3)_6^{3+}$ (mentioned in procedure 1 of Experimental Section). Initially, from the absorption spectra, this impurity was considered most likely to be either ruthenium red^{17a} ($\lambda_{\text{max}} \sim 550$ nm) or the monoterpyridine complex of ruthenium(II)⁸ ($\lambda_{\text{max}} \sim 548$ nm). Several experiments were performed in an attempt to clarify this issue. Ruthenium red was synthesized inside the zeolite by ion-exchange with $\text{Ru}(\text{NH}_3)_5(\text{H}_2\text{O})^{2+}$ in open air.^{17a} The absorption spectrum of the product is virtually identical with the reported spectrum.^{18a} After dissolution of the zeolite matrix in HF, the ~ 552 nm band could no longer be detected in the solution, indicating decomposition in acid, as is expected for Ru-red.^{18b} On the other hand, the HF extract of the contaminated Z-Ru(tpy)₂²⁺ sample contained the 552 nm band. Also, the resonance Raman spectrum of the sample did not match the reported RR spectrum of ruthenium red.¹⁹ So, the possibility that the contaminant is ruthenium red could be discounted. Several variations in the procedure for the preparation of a zeolite-entrapped monoterpyridine complex were investigated. In some cases, samples were heated at lower temperature (~ 80 °C) for short periods (several hours), but the pure mono-ligated species was not obtained. Variations in metal to ligand stoichiometry were tried in an attempt to make the mono-ligated species, but the same contaminated bis complex was obtained. At this point, the exact identity of this impurity is unknown and more experiments need to be performed. However, as explained earlier (procedure 2 of Experimental Section), pure Z-Ru(tpy)₂²⁺ was eventually synthesized by employing zeolite ion-exchanged with $\text{Ru}(\text{NH}_3)_5\text{H}_2\text{O}^{2+}$ in argon atmosphere as starting material.

B. Electronic Absorption and Emission Spectra. The very intense bands in the UV region can be assigned to ligand centered $\pi \rightarrow \pi^*$ transitions. The relatively intense and broad absorption band in the visible region, which is responsible for the deep red color, is due to spin allowed $d \rightarrow \pi^*$ metal to ligand charge transfer (MLCT) transitions.²⁰ At room temper-

- (17) (a) Sykora, M.; Treffert-Ziemelis, S. M.; Maruszewski, K.; Kincaid, J. R. *J. Am. Chem. Soc.*, in press. (b) Sykora, M.; Kincaid, J. R.; Dutta, P. K.; Castagnola, N. B. *J. Phys. Chem.*, submitted for publication.
 (18) (a) Verdonck, J. J.; Schoonheydt, R. A.; Jacobs, P. A. *J. Phys. Chem.* **1981**, 85, 2393. (b) Fletcher, J. M.; Greenfield, B. F.; Hardy, C. J.; Scargill, D.; Woodhead, J. L. *J. Chem. Soc.* **1961**, 2000.
 (19) Campbell, J. R.; Clark, J. H.; Griffith, W. P.; Hall, J. P. *J. Chem. Soc., Dalton Trans.* **1980**, 2228.
 (20) Stone, M.L.; Crosby, G. A. *Chem. Phys. Lett.* **1981**, 79, 169.

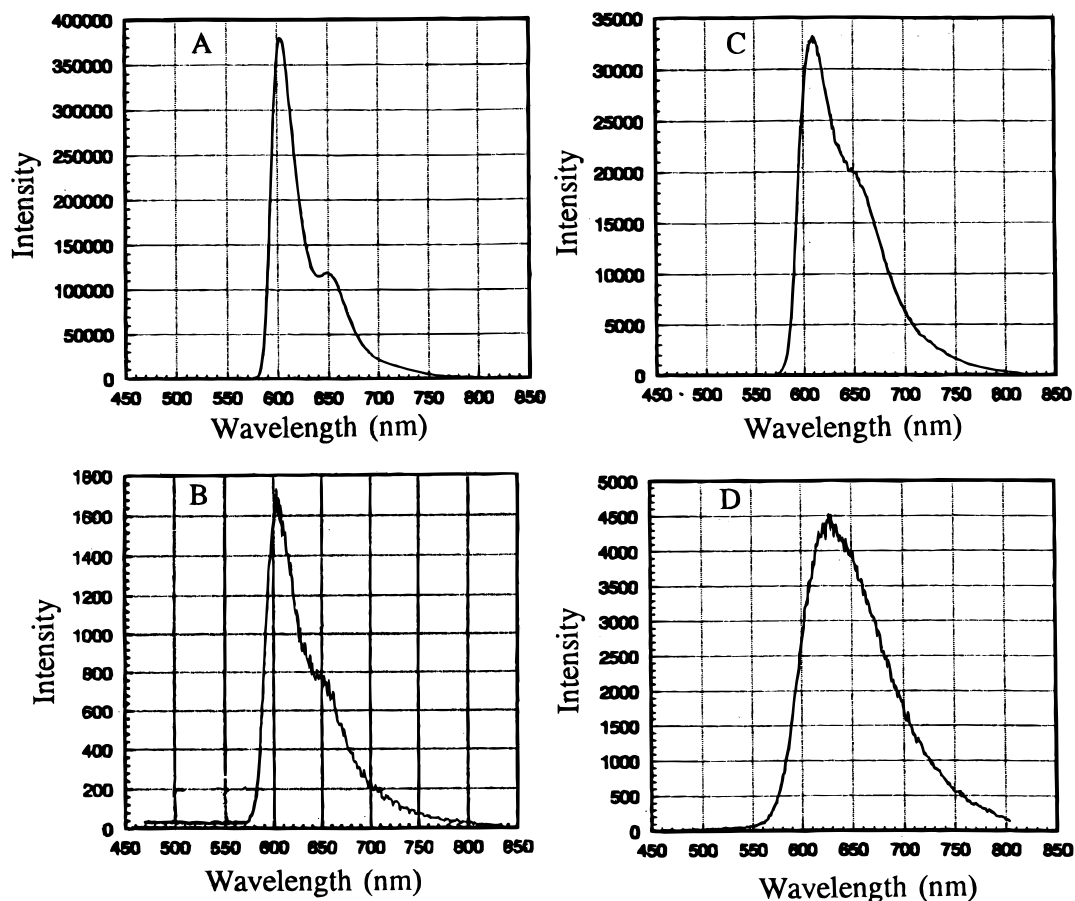


Figure 3. Electronic emission spectra of $\text{Ru}(\text{tpy})_2^{2+}$: independently synthesized complex (trace A); extracted from zeolite (trace B); zeolite-entrapped complex (trace C) at 77 K; emission of the zeolite-entrapped complex at room temperature (trace D).

ature, $\text{Ru}(\text{tpy})_2^{2+}$ is practically nonluminescent, but upon entrapment in zeolite, there is a dramatic increase in luminescence (trace d) at room temperature. In a rigid matrix at 77 K, $\text{Ru}(\text{tpy})_2^{2+}$ exhibits a strong, long-lived luminescence characteristic of a triplet¹⁴ metal to ligand charge transfer (³MLCT) level.

C. Resonance Raman (RR) Spectra. The RR spectra were obtained with excitation close to the MLCT absorption of the complex. Previous studies showed that the greatest enhancements for polypyridine modes are seen for totally symmetric vibrations between 500 and 1700 cm^{-1} .²¹ A similar type of enhancement pattern is observed for the $\text{Ru}(\text{tpy})_2^{2+}$ complex. As in the case of $\text{Ru}(\text{bpy})_3^{2+}$ and related complexes,²¹ the coordinated chelate ligands are vibrationally isolated from one another and the vibrational spectra can be satisfactorily analyzed within the framework of a single coordinated ligand of C_{2v} symmetry. While proper analysis of the vibrational spectrum will require a more extensive data set, including spectra of specifically deuterated analogues, it is interesting to compare the RR spectrum of $\text{Ru}(\text{tpy})_2^{2+}$ (Figure 4A) with the well-documented spectrum of $\text{Ru}(\text{bpy})_3^{2+}$.²¹ Thus, as has been previously noted by other workers,^{8,22} the spectrum of $\text{Ru}(\text{tpy})_2^{2+}$ appears to be a composite of modes associated with the center pyridine fragment (i.e., those occurring at 1551, 1471, 1166, and 729 cm^{-1}), which lies along the principal C_2 axis, and a set of modes involving correlated motions of the two

terminal pyridine fragments, this latter set having frequencies and relative intensities comparable to those obtained for $\text{Ru}(\text{bpy})_3^{2+}$.²¹

As was observed previously for $\text{Ru}(\text{bpy})_3^{2+}$ and related trispolypyridine complexes, entrapment of the complex within the zeolite supercages has little effect on the ground-state structure as reflected by nonsubstantial shifts in the RR enhanced vibrational modes.^{3,5,17} As can be seen by comparison of traces A and B in Figure 4, also relatively small shifts are observed for the $\text{Ru}(\text{tpy})_2^{2+}$ upon entrapment, the largest changes being observed for the modes at 1471 cm^{-1} (+6 cm^{-1}), 1018 cm^{-1} (+7 cm^{-1}), and 729 cm^{-1} (+5 cm^{-1}). Though more detailed RR studies of $\text{Ru}(\text{tpy})_2^{2+}$ and specifically deuterated analogues will be needed before such shifts can be confidently associated with specific fragments of the structure, it is interesting to note that the most significant shifts are observed for those modes thought to be ascribable to the center pyridine fragment.

D. Temperature Dependence of Lifetimes. As is summarized in Figure 1, the lowest energy ³MLCT states of ruthenium(II)–polypyridine complexes may relax to the ground state via a number of pathways, including population of two thermally accessible upper states, whose participation can be documented by analysis of lifetime data acquired over a range of temperatures.^{12,23} For most cases,¹² a single thermal term (eq 2) is adequate to fit the experimental temperature-dependent lifetime data, but in some cases,^{5b,c,23} it is necessary to use two thermal terms (eq 1) in order to fit the experimental data. The

(21) (a) Danzer, G.; Kincaid, J. J. *Phys. Chem.* **1990**, *94*, 3976. (b) Danzer, G.; Golus, J.; Kincaid, J. J. *Am. Chem. Soc.* **1993**, *115*, 8643.
(22) Schneider, S.; Brehm, G.; Prenzel, C.; Jager, W.; Silva, M.; Burrows, H.; Formosinho, S. *J. Raman Spectrosc.* **1996**, *28*, 163.

(23) Sykora, M.; Kincaid, J. R. *Inorg. Chem.* **1995**, *34*, 5852.

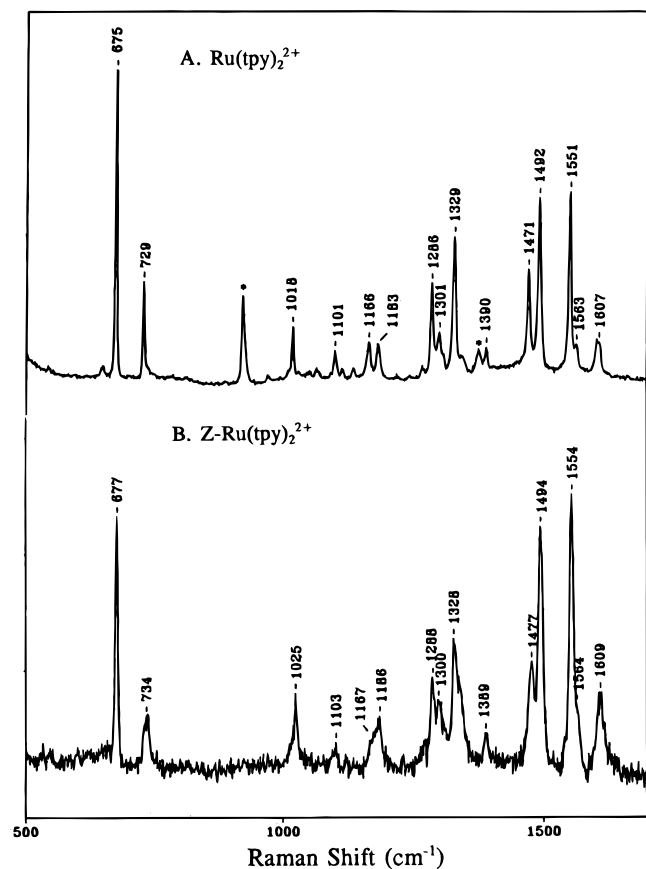


Figure 4. Resonance Raman spectra (with 476.5-nm excitation) of $\text{Ru}(\text{tpy})_2^{2+}$, independently prepared (trace A) entrapped in zeolite (trace B). Asterisks denote peaks associated with the CH_3CN solvent.

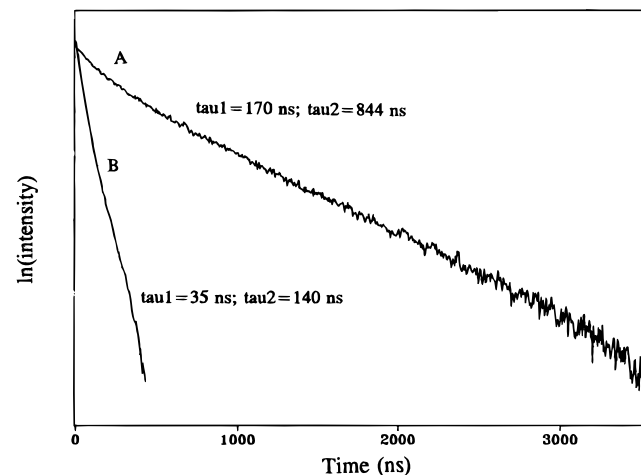


Figure 5. Logarithmic plots of the emission decay curves obtained for $\text{Z-Ru}(\text{tpy})_2^{2+}$ at $-50\text{ }^\circ\text{C}$ (trace A) and at $22\text{ }^\circ\text{C}$ (trace B). The decay curves possess biexponential character.

excited-state lifetimes (τ) are given by

$$1/\tau = k_{\text{total}} = k_r + k_{\text{nr}} + k_{\text{dd}} \exp(-\Delta E_{\text{dd}}/kT) + k_{\text{fourth}} \exp(-\Delta E_{\text{fourth}}/kT) \quad (1)$$

$$1/\tau = k_{\text{total}} = k_r + k_{\text{nr}} + k_{\text{dd}} \exp(-\Delta E_{\text{dd}}/kT) \quad (2)$$

In eqs 1 and 2, k_r and k_{nr} are the rate constants for direct radiative and nonradiative decay, respectively. The deactivation rate constant of the thermally populated (^3dd) states is designated k_{dd} . ΔE_{dd} is the energy gap between the ^3dd states and the 3 -

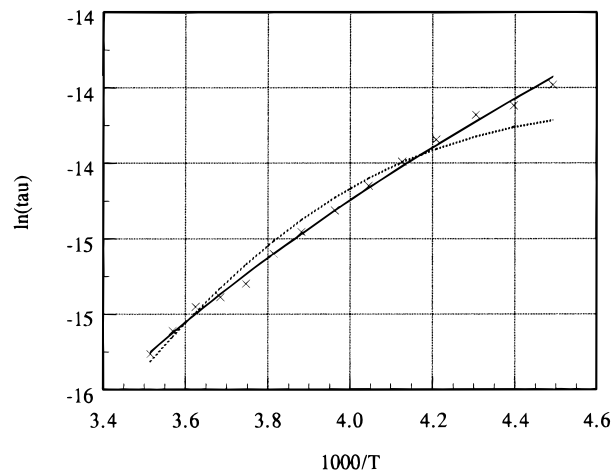


Figure 6. Temperature-dependent lifetime data obtained for $\text{Z-Ru}(\text{tpy})_2^{2+}$. The experimental points are marked by “+”. The solid line was generated from eq 1 using two thermal terms; the dotted line was obtained from eq 2 with one thermal term.

Table 1. Kinetic Decay Parameters for $\text{Ru}(\text{tpy})_2^{2+}$ Complex

compound	$k_r + k_{\text{nr}}$ (s^{-1})	k_{dd} (s^{-1})	ΔE_{dd} (cm^{-1})	k_{4th} (s^{-1})	ΔE_{4th} (cm^{-1})
$\text{Ru}(\text{tpy})_2^{2+}$ ^a	1.2×10^5	1.9×10^{13}	1500		
$\text{Z-Ru}(\text{tpy})_2^{2+}$ ^b	1.5×10^5	9.3×10^{11}	2681	3.9×10^8	929
$\text{Z-Ru}(\text{tpy})_2^{2+}$ ^c	1.3×10^6	4.5×10^{11}	2306		

^a In EtOH/MeOH; from ref 9. ^b Entrapped in zeolite; fitted using two thermal terms. ^c Entrapped in zeolite; fitted using one thermal term.

MLCT emitting states. The deactivation rate constant, k_{fourth} , is associated with an additional low lying $^3\text{MLCT}$ state (the so-called fourth MLCT state²⁴) which may be thermally populated as a consequence of the small magnitude of ΔE_{fourth} (typically $600\text{--}900\text{ cm}^{-1}$).^{5b,12,23}

In the model used for fitting of the observed lifetimes, the temperature-independent terms (k_r and k_{nr}) were replaced by a single linear term k_o . Both the equations were tested in an attempt to reproduce the observed data. One of them contained the linear term k_o and a single exponential term (eq 2) while the other possessed the linear term and both temperature-dependent terms (eq 1). Figure 6 presents the results of the fitting. Analysis of the curves shown in Figure 6 reveals that the monoexponential model (single thermal term) does not satisfactorily reproduce the observed lifetime data. However, introduction of the second thermal term yields excellent agreement between the calculated and observed curves. The long component of the lifetimes were used for fitting of the temperature-dependence of the lifetimes and for calculation of the kinetic parameters. However, the fitting of the short component also produces comparable preexponential terms and energy gaps, although a poor statistical distribution was obtained because of the low intensity of this component. The parameters for one of the derived thermal terms are $k = 9 \times 10^{11}\text{ s}^{-1}$ and $\Delta E = 2681\text{ cm}^{-1}$, values which are quite similar to those obtained for the majority of complexes which have an accessible ^3dd state. The derived parameters for the other temperature-dependent term are $k = 4 \times 10^8\text{ s}^{-1}$ and $\Delta E = 929\text{ cm}^{-1}$, the magnitudes of which are close to those previously obtained^{5b,c,12,23} for the few complexes where participation of the $^4\text{MLCT}$ state

(24) (a) Yersin, H.; Gallhuber, E.; Vogler, A.; Kunkely, H. *J. Am. Chem. Soc.* **1983**, *105*, 4155. (b) Yersin, H.; Gallhuber, E. *J. Am. Chem. Soc.* **1984**, *106*, 6582. (c) Yersin, H.; Gallhuber, E.; Hensler, G. *Chem. Phys. Lett.* **1987**, *134*, 497.

pathway dominates because the 3dd states are known to be inaccessible. Thus, it is reasonable to associate the two thermal terms with these two individual pathways.

The kinetic parameters obtained from both models are given in Table 1. Comparison of the ΔE_{dd} values for solution phase $\text{Ru}(\text{tpy})_2^{2+}$ and the zeolite-entrapped complex shows a substantial increase upon zeolite entrapment (1181 cm^{-1}). This observation accounts for the dramatic increase in lifetime and emission intensity upon zeolite entrapment. The steric constraint

induced by the rigid zeolite cage on the electronically excited $\text{Z-Ru}(\text{tpy})_2^{2+}$ results in destabilization of the LF state,^{5b} leading to a decrease in thermal population of this state.

Acknowledgment. This work was supported by a grant from the Division of Chemical Sciences, U.S. Department of Energy (Grant DE-FG 02-86ER 13619).

IC970950U